gCTRP3 inhibits oophorectomy-induced osteoporosis by activating the AMPK/SIRT1/Nrf2 signaling pathway in mice

XIAOJUAN ZHANG[1], DI ZHANG[2], HUAN ZHAO[3], JING QIN[1], HAO QI[2], FEIYU ZU[2], YARU ZHOU[1] and YINGZE ZHANG[4,5]

[1]Department of Endocrinology, The Third Hospital of Hebei Medical University, Shijiazhuang, Hebei 050051, P.R. China; [2]Department of Spinal Surgery, The Third Hospital of Hebei Medical University, Shijiazhuang, Hebei 050051, P.R. China; [3]Department of Obstetrics and Gynecology, The Third Hospital of Hebei Medical University, Shijiazhuang, Hebei 050051, P.R. China; [4]National Health Commission Key Laboratory of Intelligent Orthopaedic Equipment, The Third Hospital of Hebei Medical University, Shijiazhuang, Hebei 050051, P.R. China; [5]Department of Orthopedics, The Third Hospital of Hebei Medical University, Shijiazhuang, Hebei 050051, P.R. China

Received December 27, 2023; Accepted April 10, 2024

DOI: 10.3892/mmr.2024.13257

Abstract. C1q/tumor necrosis factor-related protein 3 (CTRP3) expression is markedly reduced in the serum of patients with osteoporosis. The present study aimed to investigate whether CTRP3 reduces bone loss in oophorectomy (OVX)-induced mice via the AMP-activated protein kinase (AMPK)/sirtuin 1 (SIRT1)/nuclear factor E2-related factor 2 (Nrf2) signaling pathway. Female C57BL/6J mice and MC3T3-E1 cells were used to construct *in vivo* and *in vitro* models of osteoporosis, respectively. The left femurs of mice were examined using micro-computed tomography scans and bone-related quantitative morphological evaluation was performed. Pathological changes and the number of osteoclasts in the left femurs of mice were detected using hematoxylin and eosin, and tartrate-resistant acid phosphatase (TRAP) staining. Runt-related transcription factor-2 (RUNX2) expression in the left femurs was detected using immunofluorescence analysis, and the serum levels of bone resorption markers (C-telopeptide of type I collagen and TRAP) and bone formation markers [osteocalcin (OCN) and procollagen type 1 N-terminal propeptide] were detected. In addition, osteoblast differentiation and calcium deposits were examined in MC3T3-E1 cells using alkaline phosphatase (ALP) and Alizarin red staining, respectively. Moreover, *RUNX2*, *ALP* and *OCN* expression levels were detected using reverse transcription-quantitative PCR, and the expression levels of proteins associated with the AMPK/SIRT1/Nrf2 signaling pathway were detected using western blot analysis. The results revealed that globular CTRP3 (gCTRP3) alleviated bone loss and promoted bone formation in OVX-induced mice. gCTRP3 also facilitated the osteogenic differentiation of MC3T3-E1 cells through the AMPK/SIRT1/Nrf2 signaling pathway. The addition of an AMPK inhibitor (Compound C), SIRT1 inhibitor (EX527) or Nrf2 inhibitor (ML385) reduced the osteogenic differentiation of MC3T3-E1 cells via inhibition of gCTRP3. In conclusion, gCTRP3 inhibits OVX-induced osteoporosis by activating the AMPK/SIRT1/Nrf2 signaling pathway.

Correspondence to: Professor Yingze Zhang, Department of Orthopedics, The Third Hospital of Hebei Medical University, 139 Ziqiang Road, Qiaoxi, Shijiazhuang, Hebei 050051, P.R. China
E-mail: yzzhang0311@126.com

Key words: gCTRP3, osteoporosis, oophorectomy, AMPK/SIRT1/Nrf2 signaling pathway

Introduction

Primary osteoporosis is a metabolic disease in which bone loss leads to increased bone fragility; notably, this condition is more common in postmenopausal women (1). The rate of bone formation is lower than the rate of bone resorption by osteoclasts, which ultimately leads to osteoporosis (2). Further investigations into potential indicators of osteoporosis are required, to improve the timely diagnosis of osteoporosis and to reduce the probability of fracture in clinical practice.

C1q/tumor necrosis factor-related protein-3 (CTRP3) is a highly hydrophilic secreted protein that serves an important role in a variety of metabolic and inflammatory diseases (3-5). Serum CTRP3 levels have been shown to be decreased in patients with osteoporosis, and a significant decrease in the incidence of osteoporosis has been observed in the presence of CTRP3 (6). The results of a previous study demonstrated that the serum levels of CTRP3 in patients with primary hyperparathyroidism are lower than those observed in healthy controls (7). In addition, the serum levels of CTRP3 in patients with primary hyperparathyroidism with osteoporosis were shown to be lower than those in patients with primary hyperparathyroidism without osteoporosis. The results of a logistic regression analysis further revealed that CTRP3 levels may be used to independently determine whether a patient has osteoporosis (7). However, the specific role of CTRP3 in osteoporosis has yet to be fully elucidated. CTRP3 is highly upregulated in fracture callus tissue, and delayed intrachondral fracture healing can lead to abnormal mineral distribution

in CTRP3-knockout mice. By contrast, callus remodeling has been reported to be accelerated in mice with CTRP3 overexpression (8). The results of a previous study also revealed that CTRP3 suppresses osteoclastogenic factor-induced osteoclast differentiation and bone destruction (9). Notably, CTRP3 significantly accelerates the calcification of abdominal aorta and the arterial ring, upregulates the expression of osteogenic marker genes, and enhances the expression of osteogenic markers in β-glycerophosphate-induced vascular smooth muscle cells (10). The results of these previous studies highlighted that CTRP3 exhibits a specific regulatory effect on the differentiation of osteoblasts and osteoclasts. Activation of the AMP-activated protein kinase (AMPK)/sirtuin 1 (SIRT1) signaling pathway promotes the osteogenic differentiation and antioxidant response of mouse bone mesenchymal stem cells (11), and activation of AMPK/nuclear factor estradiol (E2)-related factor 2 (Nrf2) inhibits RANKL-induced osteoclast generation and oxidative stress (12). Therefore, it was hypothesized that CTRP3 may inhibit oophorectomy (OVX)-induced bone loss in mice, and this process may be associated with the AMPK/SIRT1/Nrf2 signaling pathway.

Globular CTRP3 (gCTRP3) is a truncated form of CTRP3, and is termed 'globular' because it comprises the C-terminal globular domain of CTRP3 (13). CTRPs all contain C1q globular domains and are jointly characterized as the 1q/TNF superfamily, which comprises CTRP1, CTRP3, CTRP4, CTRP5, CTRP6 and CTRP7 (14-16). Notably, the globular structure of CTRP1 has been proven to be consistent with the function of the full-length domain of CTRP1 (17). As previously described, gCTRP3 is biologically active, and gCTRP3 has been demonstrated to improve impaired vasodilatation of microvasculature in diabetes by ameliorating endothelial cell function (13). Besides, supplementation with the recombinant human gCTRP3 protects against high-fat diet-induced spermatogenic deficiency in mice (18). gCTRP3 has been reported to promote mitochondrial biogenesis in hypoxia/reoxygenation-induced rat cardiomyocytes (19). A recent study demonstrated that gCTRP3 treatment improves impaired vasodilatation of the microvasculature in a murine model of type 2 diabetes mellitus by ameliorating endothelial cell function (13). The present study aimed to explore the effects of gCTRP3 on OVX-induced mice, and MC3T3-E1 cells were selected for *in vitro* experiments in this study. The MC3T3-E1 mouse calvaria-derived preosteoblast cell line has contributed to the investigation of the role of osteoblasts in bone formation (20). In addition, the role of AMPK/SIRT1/Nrf2 signaling was investigated using an AMPK inhibitor (Compound C), SIRT1 inhibitor (EX527) and Nrf2 inhibitor (ML385).

Materials and methods

Animal experiments. A total of 30 female C57BL/6J mice (age, 6 weeks; weight, 21-25 g) purchased from Hangzhou Ziyuan Laboratory Animal Technology Co., Ltd. were housed under the conditions of a 12-h light/dark cycle at 21-23˚C with a relative humidity of 60-65% with free access to water and food. All experimental procedures were carried out according to institutional guidelines and were approved by the Animal Care and Ethics Committee of The Third Hospital of Hebei Medical University (Shijiazhuang, China; approval no. Z2023-020-1). All mice were anesthetized using an intraperitoneal injection of 50 mg/kg sodium pentobarbital. OVX was achieved through removal of the bilateral ovaries, and an equal amount of adipose tissue was removed to create control-operated mice.

At 1 week post-surgery, the control-operated mice were randomly divided into the following two groups (n=6/group): i) Control group (control-operated mice treated with distilled water) and ii) gCTRP3 group [control-operated mice treated with human recombinant gCTRP3 (0.5 mg/kg)]. The OVX mice were randomly divided into the following three groups (n=6/group): i) OVX group (OVX mice treated with distilled water); ii) OVX + gCTRP3 group [OVX mice treated with gCTRP3 (0.5 mg/kg)]; and iii) OVX + E2 group [OVX mice treated with E2-valerate tablets (Bayer Healthcare Co., Ltd.; 1 mg/kg)]. Mice in the treatment groups were administered gCTRP3, E2 or an equal volume of distilled water once a day via gavage. gCTRP3 was purchased from Aviscera Bioscience. After 12 weeks of treatment, all mice were fasted overnight and euthanized with an intraperitoneal injection of 200 mg/kg sodium pentobarbital. Subsequently, blood was collected from the femoral artery, and serum was obtained following the centrifugation of blood at 1,000 x g for 10 min at 4˚C. The left femurs of all mice were isolated for micro-computed tomography (CT) and histological analysis.

Micro-CT scans and histological analysis. For micro-CT scans, the left femurs were evaluated using a Skyscan 1076 scanner (SkyScan NV) at 35 μm resolution. Reconstructed images were segmented to quantify the trabecular bone structure using CTAn software (v1.10.9.0; SkyScan NV), and 3D images were visualized using Ant software (release 2.05; SkyScan NV). The volume of interest (VOI) was 1-1.5 mm below the growth plate. The bone mineral density (BMD), bone volume/tissue volume (BV/TV), trabecular number (Tb.N), trabecular thickness (Tb.Th) and trabecular spacing (Tb.Sp) were calculated within the delimited VOI (21). For histological analysis, the left femurs were fixed in 4% paraformaldehyde for 24 h at room temperature, decalcified in 12% EDTA (pH 7.4) for 21 days at room temperature, and embedded in paraffin. The tissues were sliced into 5-μm sections, and these were subsequently used for hematoxylin and eosin, and tartrate-resistant acid phosphatase (TRAP) staining. For hematoxylin and eosin staining, the sections were stained with hematoxylin for 5 min at room temperature and eosin for 5 min at room temperature. TRAP staining was performed using a 387A kit (Merck KGaA), Briefly, a mixed solution of citrate solution, Fast Gamet GBC Base solution, naphthol AS-BI phosphonic acid solution and sodium nitrite solution were preheated at 37˚C before tartrate solution was added to the mixture, the sections were then submerged into the mixed solution for 1 h at 37˚C. Stained sections were photomicrographed using a light microscope (Olympus Corp.).

Immunofluorescence analysis. The paraffin-embedded sections (5 μm) were dewaxed with xylene and rehydrated with a gradient ethanol series. The sections were then permeabilized with 0.1% Triton X-100 (BioFroxx; neoFroxx GmbH) for 3 min followed by incubation with 5% bovine serum albumin (BSA; BioFroxx; neoFroxx GmbH) for 1 h at room temperature. Subsequently, the sections were incubated with

an anti-Runt-related transcription factor-2 (RUNX2) antibody (1:10,000; cat. no. 12556S; Cell Signaling Technology, Inc.) overnight at 4˚C. Subsequently, sections were washed with PBS and incubated with goat anti-rabbit IgG secondary antibody conjugated to Alexa Fluor® 488 (1:1,000; cat. no. 4412S; Cell Signaling Technology, Inc.) at room temperature for 1 h. After washing in PBS, the sections were counterstained with DAPI for 10 min at room temperature and were observed under a fluorescence microscope (Olympus Corp.).

ELISA. The levels of C-telopeptide of type I collagen (CTX-1), TRAP, osteocalcin (OCN) and procollagen type 1 N-terminal propeptide (P1NP) in serum were detected using CTX-1 (cat. no. E-EL-M3023; Elabscience Biotechnology, Inc.), TRAP (cat. no. SP14794; SPBIO), OCN (cat. no. E-EL-M0864c; Elabscience Biotechnology, Inc.) and P1NP (cat. no. E-EL-M0233c; Elabscience Biotechnology, Inc.) ELISA kits according to the manufacturers' instructions. Absorbance was measured using a microplate reader.

Cell culture and treatment. MC3T3-E1 cells (cat. no. CRL-2593) were obtained from the American Type Culture Collection, and were cultured in α-MEM (HyClone; Cytiva) supplemented with 10% FBS (HyClone; Cytiva), 100 U/ml penicillin and 100 μg/ml streptomycin at 37˚C with 5% CO_2. Prior to osteogenic differentiation, MC3T3-E1 cells were pretreated with different concentrations of gCTRP3 (0.2, 1 and 2 μg/ml) for 24 h at 37˚C. An AMPK inhibitor (Compound C; 1 μM; MedChemExpress) (22), SIRT1 inhibitor (EX527; 10 μM; MedChemExpress) (23) or Nrf2 inhibitor (ML385; 5 μM; MedChemExpress) (24) was used to treat MC3T3-E1 cells in the presence of gCTRP3 for 24 h at 37˚C. Subsequently, MC3T3-E1 cells were seeded into 6-well plates at a density of $1x10^4$ cells/well and cultured in α-MEM supplemented with 10 mM β-glycerol phosphate, 50 μg/ml ascorbic acid and 100 nM dexamethasone for up to 14 days at 37˚C.

Cell Counting Kit-8 (CCK-8) assay. The viability of MC3T3-E1 cells was evaluated using a CCK-8 assay kit (Beijing Solarbio Science & Technology Co., Ltd.). Following pretreatment with gCTRP3, MC3T3-E1 cells were incubated with CCK-8 solution (10 μl) for 2 h at 37˚C. Absorbance was detected using a microplate reader at a wavelength of 450 nm.

Alkaline phosphatase (ALP) activity. The ALP activity of MC3T3-E1 cells was detected using an ALP assay kit (cat. no. E-BC-K091-S; Elabscience Biotechnology, Inc.) according to the manufacturer's instructions. Absorbance was detected using a microplate reader at a wavelength of 450 nm.

ALP staining and Alizarin red staining (ARS). For ALP staining, MC3T3-E1 cells were fixed with 4% formaldehyde at room temperature for 30 min, rinsed with 0.05% TBS supplemented with Tween-20 and stained with naphthol/Fast Red Violet solution (Sigma-Aldrich; Merck KGaA) at room temperature for 15 min, according to the manufacturer's instructions. Then cells were rinsed and imaged under a light microscope (Olympus Corp.).

For ARS, MC3T3-E1 cells were fixed with 4% formaldehyde at room temperature for 15 min and stained with 40 mM ARS dye (pH 4.2; Beyotime Institute of Biotechnology) at room temperature for 10 min. Calcium deposits were observed under a light microscope (Olympus Corp.).

Reverse transcription-quantitative PCR (RT-qPCR). Following treatment, total RNA was extracted from MC3T3-E1 cells using TRIzol® reagent (Invitrogen; Thermo Fisher Scientific, Inc.). RNA was reverse transcribed into cDNA using the PrimeScript RT reagent kit (Takara Bio, Inc.) according to manufacturer's protocol, followed by qPCR using Kapa SYBR® FAST qPCR Master Mix (Takara Bio, Inc.). The PCR reaction conditions consisted of 95˚C for 3 min, followed by 40 cycles of 95˚C for 30 sec and 60˚C for 30 sec. *RUNX2*, *ALP* and *OCN* mRNA expression levels in MC3T3-E1 cells were quantified using the $2^{-\Delta\Delta Cq}$ method and normalized to the internal reference gene *GAPDH* (25). The primer sequences were designed by Sangon Biotech Co., Ltd. The following primer pairs were used for qPCR: *RUNX2*, forward 5'-GCCAATCCCTAAGTGTGG CT-3', reverse 5'-AACAGAGAGCGAGGGGGTAT-3'; *ALP*, forward 5'-TGGTCACAGCAGTTGGTAGC-3', reverse 5'-CTG AGATTCGTCCCTCGCTG-3'; *OCN*, forward 5'-ATGGCT TGAAGACCGCCTAC-3', reverse 5'-GACAGGGAGGATCAA GTCCC-3'; and *GAPDH*, forward 5'-CCCTTAAGAGGGATG CTGCC-3' and reverse 5'-TACGGCCAAATCCGTTCACA-3'.

Western blot analysis. Following treatment, MC3T3-E1 cells were lysed in ice-cold RIPA lysis buffer (Beyotime Institute of Biotechnology). The concentration of total proteins in MC3T3-E1 cells was detected using a BCA protein assay kit (Beyotime Institute of Biotechnology). Equal amounts of protein (40 μg per lane) were separated by SDS-PAGE on 10% gels and were transferred onto polyvinylidene difluoride membranes. After blocking with 5% BSA for 1 h at room temperature, the membranes were incubated with primary antibodies against phosphorylated (p)-AMPK (1:1,000 dilution; cat. no. 2535T; Cell Signaling Technology, Inc.), AMPK (1:1,000; cat. no. 2532S; Cell Signaling Technology, Inc.), SIRT1 (1:1,000; cat. no. 9475T; Cell Signaling Technology, Inc.), Nrf2 (1:1,000; cat. no. 80593-1-RR; Proteintech Group, Inc.) and GAPDH (1:1,000; cat. no. 2118T; Cell Signaling Technology, Inc.) overnight at 4˚C. Subsequently, the membranes were incubated with HRP-conjugated goat anti-rabbit IgG secondary antibody (1:10,000; cat. no. 7074P2; Cell Signaling Technology, Inc.) for 1 h at room temperature. Protein bands were visualized using ECL reagent (MilliporeSigma) and protein expression was semi-quantified using ImageJ (version 1.8.0; National Institutes of Health).

Statistical analysis. All experiments were independently repeated three times and data are presented as the mean ± standard deviation. Statistical analyses were performed using GraphPad Prism software (version 8.0.1; Dotmatics). One-way ANOVA followed by Tukey's post-hoc test was used to compare differences among multiple groups. $P<0.05$ was considered to indicate a statistically significant difference.

Results

gCTRP3 treatment alleviates bone loss in OVX-induced mice. Results of the micro-CT scan demonstrated that loss

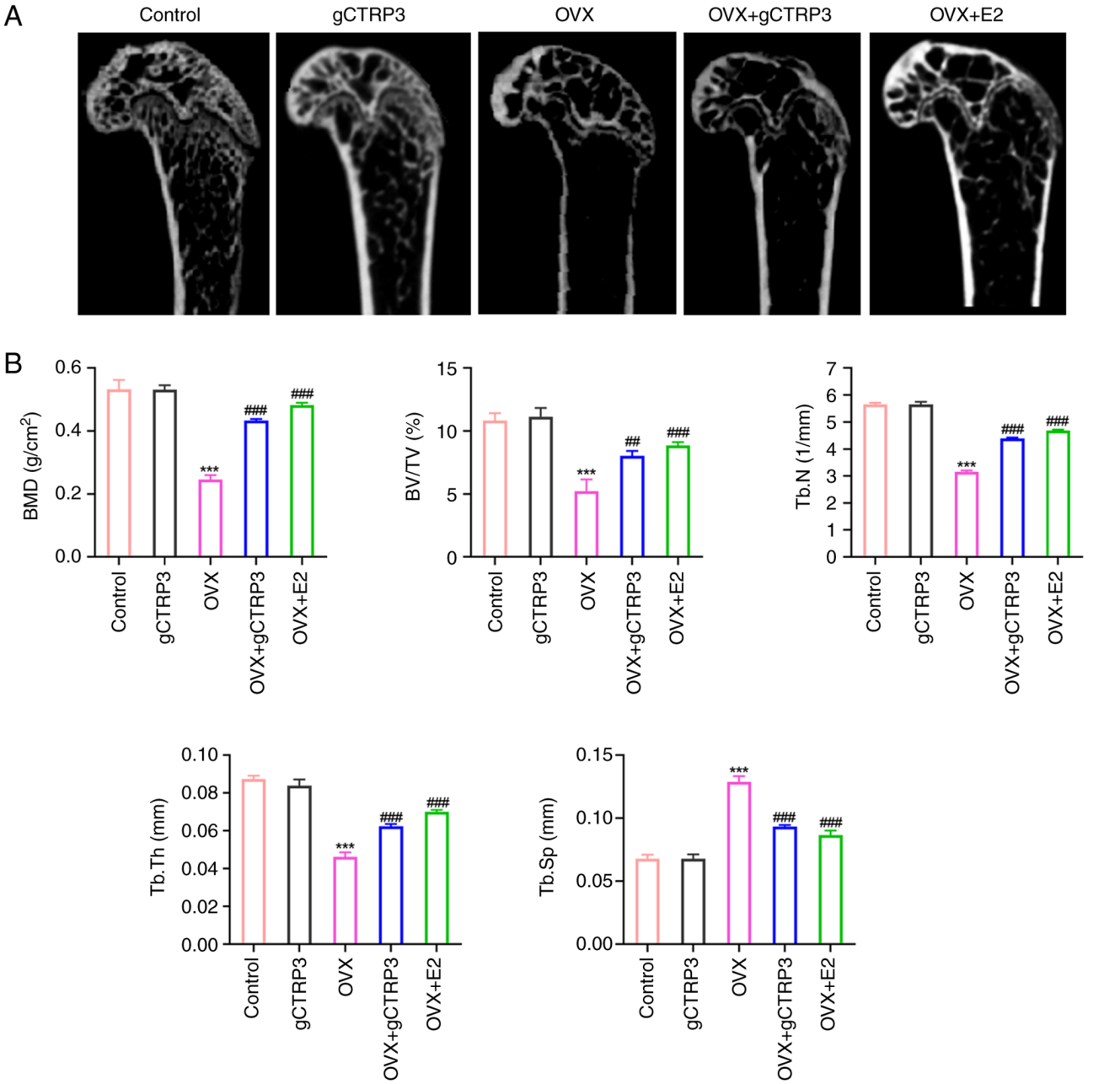

Figure 1. gCTRP3 alleviates bone loss in OVX-induced mice. (A) Left femurs of OVX-induced mice were examined using a micro-computed tomography scan following gCTRP3 treatment. (B) BMD, BV/TV, Tb.N, Tb.Th and Tb.Sp were quantified in the left femurs of OVX-induced mice following treatment with gCTRP3. ***P<0.001 vs. Control group; $^{\#\#}$P<0.01, $^{\#\#\#}$P<0.001 vs. OVX group. gCTRP3, globular C1q/tumor necrosis factor-related protein 3; OVX, oophorectomy; E2, estradiol valerate; BMD, bone mineral density; BV/TV, bone volume/tissue volume; Tb.N, trabecular number; Tb.Th, trabecular thickness; Tb.Sp, trabecular separation.

of the trabecular bone occurred in OVX-induced mice, and this loss was improved in mice treated with gCTRP3 and E2 (the positive drug group) (Fig. 1A). Morphometric analysis of the left femurs of OVX-induced mice demonstrated that BMD, BV/TV, Tb.N and Tb.Th were decreased in OVX-induced mice, and these levels were markedly restored following treatment with gCTRP3 and E2 (Fig. 1B). By contrast, Tb.Sp was increased in OVX-induced mice, and this was decreased following treatment with gCTRP3 and E2 (Fig. 1B). Notably, the cortical bone thickness and trabecular area were markedly decreased in OVX-induced mice; however, the bone mass of OVX-induced mice was increased in the gCTRP3 and E2 group (Fig. 2A). In addition, TRAP staining indicated that OVX induced an increase in the number of osteoclasts, and this number was decreased following treatment with gCTRP3 and E2 (Fig. 2B). In addition, the expression levels of RUNX2, a marker of bone formation, were reduced in OVX-induced mice, and treatment with gCTRP3 and E2 increased the expression levels (Fig. 2C). Simultaneously, the serum levels of bone resorption markers (CTX-1 and TRAP) were increased, and those of bone formation markers (OCN and P1NP) were decreased in OVX-induced mice (Fig. 2D), which was consistent with the results of previous studies (26-28). By contrast, these

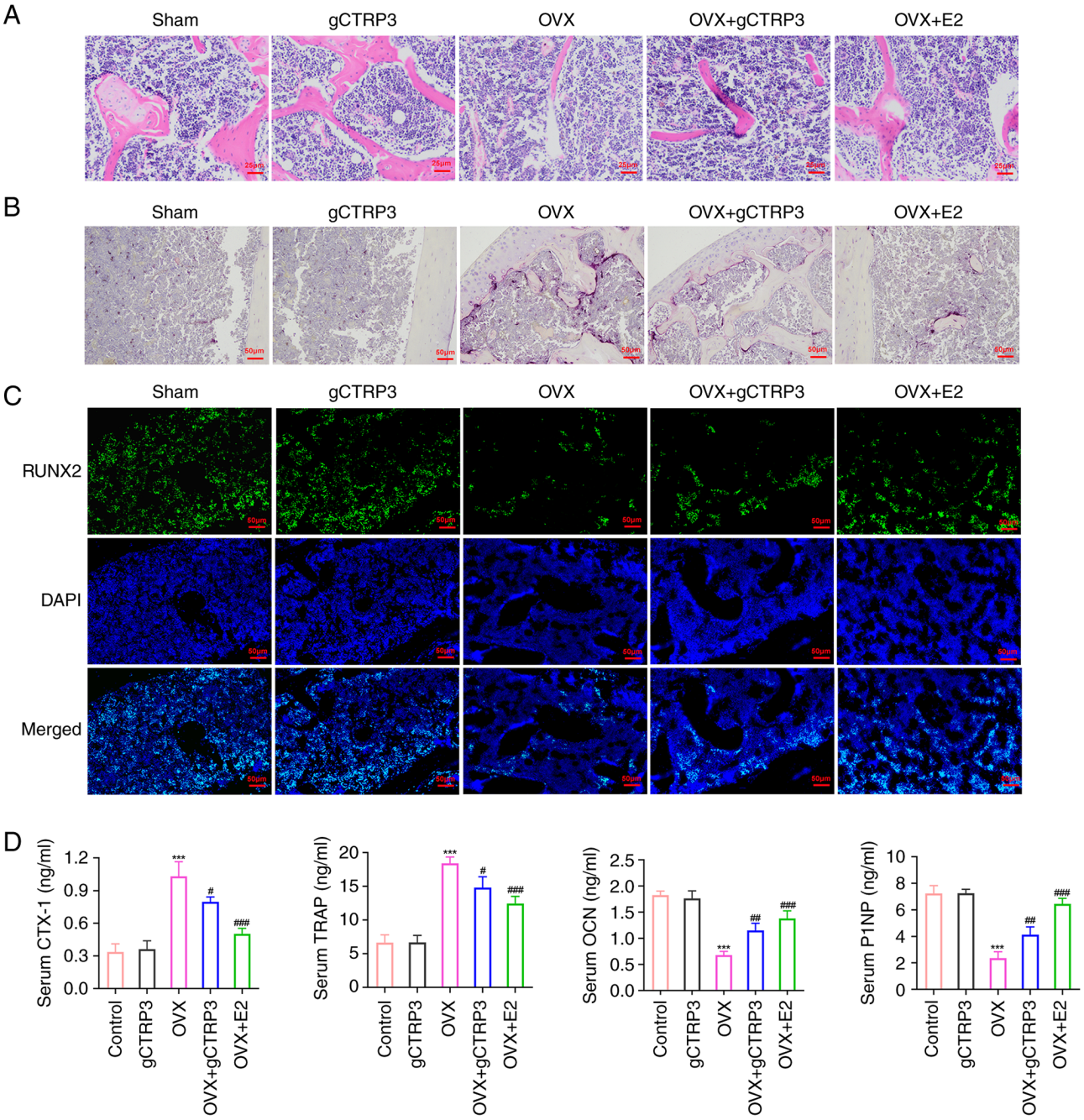

Figure 2. gCTRP3 inhibits bone resorption and promotes bone formation. (A) Pathological changes of the left femurs of OVX-induced mice were observed using hematoxylin and eosin staining following treatment with gCTRP3 (scale bar, 25 μm). (B) Number of osteoclasts in the left femurs of OVX-induced mice were observed using TRAP staining following treatment with gCTRP3 (scale bar, 50 μm). (C) RUNX2 expression levels in the left femurs of OVX-induced mice were detected using immunofluorescence analysis following treatment with gCTRP3 (scale bar, 50 μm). (D) CTX-1, TRAP, OCN and P1NP expression levels in the serum of OVX-induced mice were detected using ELISA kits following treatment with gCTRP3. ***P<0.001 vs. Control group; $^{\#}$P<0.05, $^{\#\#}$P<0.01 and $^{\#\#\#}$P<0.001 vs. OVX group. gCTRP3, globular C1q/tumor necrosis factor-related protein 3; OVX, oophorectomy; E2, estradiol valerate; TRAP, tartrate-resistant acid phosphatase; RUNX2, Runt-related transcription factor-2; CTX-1, C-telopeptide of type I collagen; OCN, osteocalcin; P1NP, procollagen type 1 N-terminal propeptide.

levels were restored following treatment with gCTRP3 and E2 (Fig. 2D). Collectively, the results of the present study demonstrated that gCTRP3 treatment alleviated bone loss in OVX-induced mice.

gCTRP3 promotes the osteogenic differentiation of MC3T3-E1 cells. As shown in Fig. 3A, different concentrations of gCTRP3 did not affect the viability of MC3T3-E1 cells, compared with that in the untreated control group. Furthermore, ALP activity, osteoblast differentiation and mineralized calcium nodules were all increased following treatment with gCTRP3 from 0.2 to 2 μg/ml, when compared with the control group (Fig. 3B-D). Consistently, *RUNX2*, *ALP* and *OCN* expression levels were increased in MC3T3-E1 cells following treatment with gCTRP3 from 0.2 to 2 μg/ml (Fig. 3E). Collectively, the results of the present study suggested that gCTRP3 may promote the osteogenic differentiation of MC3T3-E1 cells.

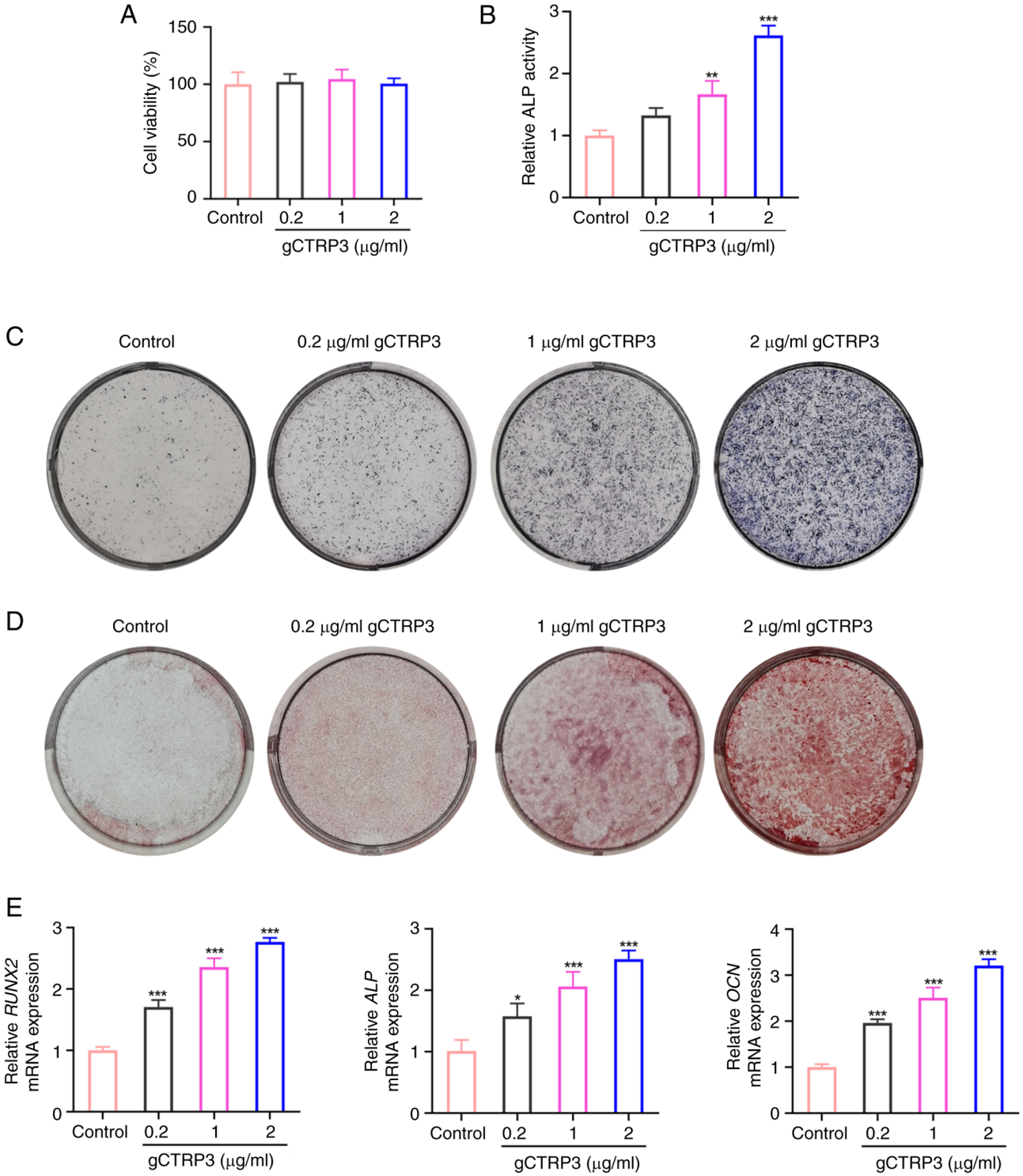

Figure 3. gCTRP3 promotes the osteogenic differentiation of MC3T3-E1 cells. (A) MC3T3-E1 cell viability was detected using a Cell Counting Kit-8 assay following treatment with different concentrations of gCTRP3. (B) ALP activity of MC3T3-E1 cells was detected using an ALP assay kit following treatment with different concentrations of gCTRP3. (C) Osteoblast differentiation of MC3T3-E1 cells was investigated using ALP staining following treatment with different concentrations of gCTRP3. (D) Calcium deposits were detected in MC3T3-E1 cells using ARS staining following treatment with different concentrations of gCTRP3. (E) Expression levels of osteogenic marker genes in MC3T3-E1 cells were detected using reverse transcription-quantitative PCR following treatment with different concentrations of gCTRP3. *P<0.05, **P<0.01 and ***P<0.001 vs. Control group. gCTRP3, globular C1q/tumor necrosis factor-related protein 3; ALP, alkaline phosphatase; ARS, Alizarin red staining; RUNX2, Runt-related transcription factor-2; OCN, osteocalcin.

gCTRP3 activates the AMPK/SIRT1/Nrf2 signaling pathway in MC3T3-E1 cells. Western blot analysis was used to evaluate the expression levels of proteins associated with AMPK/SIRT1/Nrf2 signaling in MC3T3-E1 cells, in the presence of gCTRP3. The results of the present study demonstrated that p-AMPK, SIRT1 and Nrf2 expression levels were increased in MC3T3-E1 cells following treatment with 1 and 2 μg/ml gCTRP3 (Fig. 4). By contrast, AMPK expression was not altered in MC3T3-E1 cells following treatment with different concentrations of gCTRP3 (Fig. 4).

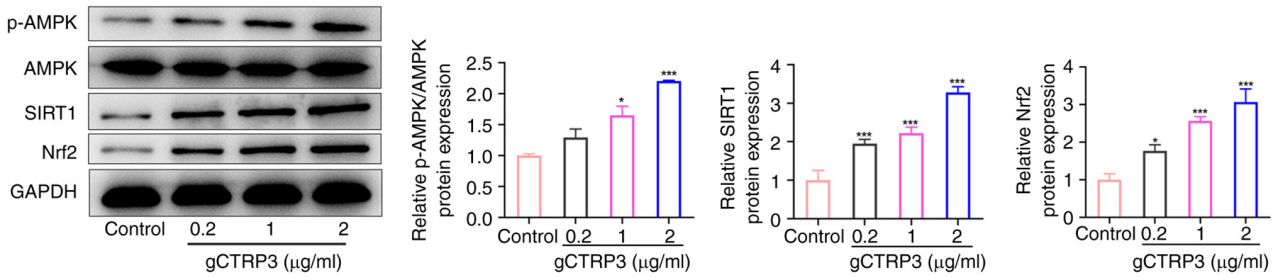

Figure 4. gCTRP3 activates the AMPK/SIRT1/Nrf2 signaling pathway. Expression levels of proteins associated with the AMPK/SIRT1/Nrf2 signaling pathway were determined in MC3T3-E1 cells following treatment with different concentrations of gCTRP3. *P<0.05 and ***P<0.001 vs. Control group. gCTRP3, globular C1q/tumor necrosis factor-related protein 3; p-, phosphorylated; AMPK, AMP-activated protein kinase; SIRT1, sirtuin 1; Nrf2, nuclear factor E2-related factor 2.

Collectively, these data revealed that gCTRP3 activates the AMPK/SIRT1/Nrf2 signaling pathway in MC3T3-E1 cells.

gCTRP3 promotes the osteogenic differentiation of MC3T3-E1 cells through activating the AMPK/SIRT1/Nrf2 signaling pathway. MC3T3-E1 cells were treated with an AMPK inhibitor (Compound C), SIRT1 inhibitor (EX527) or Nrf2 inhibitor (ML385) to assess whether gCTRP3 promoted osteogenic differentiation via the AMPK/SIRT1/Nrf2 signaling pathway. As displayed in Fig. 5A-C, gCTRP3 treatment elevated ALP activity, osteoblast differentiation and mineralized calcium nodules, whereas these factors were reduced following treatment with Compound C, EX527 and ML385. In addition, the gCTRP3-mediated increases in the expression levels of *RUNX2*, *ALP* and *OCN* were reduced following treatment with Compound C, EX527 and ML385 in MC3T3-E1 cells (Fig. 5D). Collectively, these data demonstrated that gCTRP3 promotes the osteogenic differentiation of MC3T3-E1 cells through activating the AMPK/SIRT1/Nrf2 signaling pathway.

Discussion

The results of the present study revealed that gCTRP3 alleviated bone loss in OVX-induced mice. Moreover, gCTRP3 increased BMD, BV/TV, Tb.N and Tb.Th, decreased Tb.Sp, and improved cortical bone thickness and trabecular area. The results of the present study also demonstrated that treatment with gCTRP3 decreased the number of osteoclasts, promoted the levels of RUNX2, OCN and P1NP, and inhibited the levels of CTX-1 and TRAP. *In vitro,* gCTRP3 promoted ALP activity, osteoblast differentiation and mineralized calcium nodules through activating the AMPK/SIRT1/Nrf2 signaling pathway, and these factors were reversed following treatment with Compound C, EX527 and ML385.

As a member of the CTRP family, CTRP3 is highly expressed in cartilage and adipocytes. CTRP3 participates in the proliferation and migration of chondrocytes, and regulates the homeostasis of cartilage and bone metabolism *in vivo* (7,8). In patients with reduced CTRP3 expression levels, the metabolism of calcium and phosphorus is unbalanced, and the absorption capacity of calcium, phosphorus and other substances is reduced, leading to osteoporosis (6). Maeda *et al* (29) reveled that CTRP3 may be involved in chondrocyte development. Yokohama-Tamaki *et al* (30) demonstrated that CTRP3 may be essential for mandible regulation via perichondrium maintenance and neochondrogenesis. The results of a previous study revealed that reduced CTRP3 expression inhibits the proliferation, migration and invasion of osteosarcoma cells (31). Moreover, CTRP3 can inhibit the hypoxia/serum deprivation-induced apoptosis of bone marrow-derived mesenchymal stem cells (32). The results of the present study demonstrated that gCTRP3 serves a key role in bone formation in OVX-induced mice, and promoted the ALP activity, osteoblast differentiation and mineralized calcium nodules of MC3T3-E1 cells.

ALP hydrolyzes organophosphate, increases inorganic phosphate local rates and facilitates mineralization as well as reduces the concentration of extracellular pyrophosphate, an inhibitor of mineral formation (33). In addition, ALP promotes bone calcification and acts as a prerequisite for the formation of calcium nodules (34). The expression of RUNX2 indicates the onset of osteogenic differentiation, which occurs at the earliest stage of bone formation (35). The expression of RUNX2 in bone tissue after OVX remains controversial, and may be affected by different stages of osseointegration, mouse background or various bone tissue (36-38). OCN is a non-collagen protein that is present in bone tissue, and levels are indicative of maturity during osteogenic differentiation (39). The results of the present study demonstrated that treatment with gCTRP3 significantly increased the expression levels of *ALP*, *RUNX2* and *OCN* in MC3T3-E1 cells, suggesting that gCTRP3 may promote the osteogenic differentiation of MC3T3-E1 cells.

The results of previous studies demonstrated that AMPK is a therapeutic target for metabolic diseases, cancer and atherosclerosis, which serves an important role in anti-inflammatory, antitumor and anti-aging treatments (40-43). At present, osteoporosis is considered a metabolic disease that is comparable with diabetes and obesity, and AMPK promotes osteoblast differentiation and bone formation (44). Through the AMPK signaling pathway, Si-Zhi Wan, a traditional Chinese medicine used to treat osteoporosis, inhibits osteoclast autophagy in osteoporosis to attenuate osteoclastogenesis (45). Isovaleric acid stimulates AMPK phosphorylation, and treatment with an AMPK inhibitor (Compound C) blocks isovaleric acid-induced inhibition of osteoclast generation (46). This suggests that the AMPK signaling pathway serves a key role in bone metabolism in osteoporosis. Compound C attenuates AMPK expression in different types of cells (47), and inhibits the osteogenic differentiation of cells (48,49). AMPK activation directly inhibits the generation of osteoclasts (50), stimulates the production

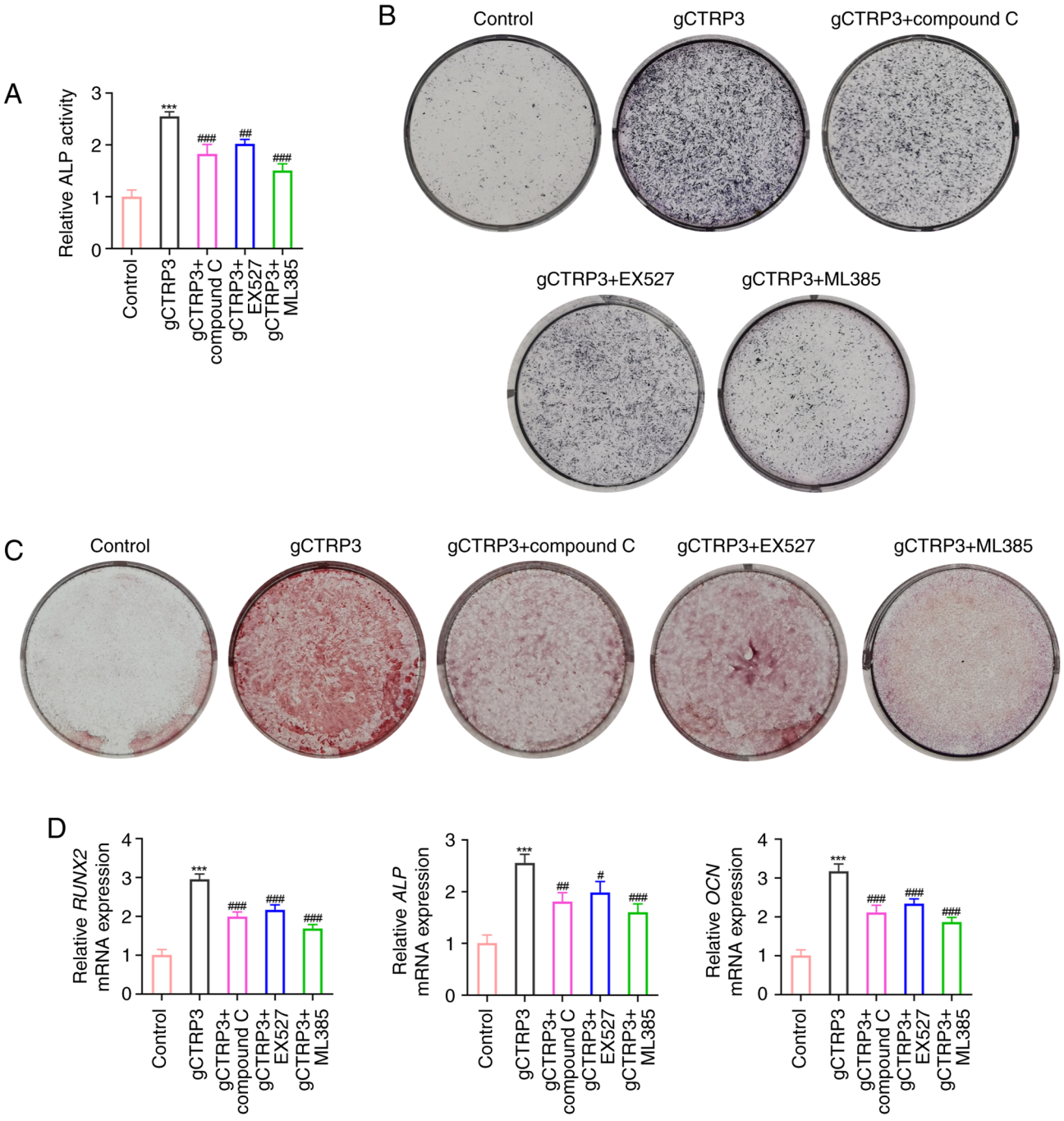

Figure 5. gCTRP3 promotes the osteogenic differentiation of MC3T3-E1 cells through the AMP-activated protein kinase/sirtuin 1/nuclear factor E2-related factor 2 signaling pathway. (A) ALP activity of MC3T3-E1 cells was detected using an ALP assay kit following treatment with gCTRP3 and a signaling pathway inhibitor. (B) Osteoblast differentiation of MC3T3-E1 cells was determined using ALP staining following treatment with gCTRP3 and a signaling pathway inhibitor. (C) Calcium deposits in MC3T3-E1 cells were determined using ARS staining following treatment with gCTRP3 and a signaling pathway inhibitor. (D) Expression levels of osteogenic marker genes were determined using reverse transcription-quantitative PCR following treatment with gCTRP3 and a signaling pathway inhibitor. ***P<0.001 vs. Control group; $^{\#}$P<0.05, $^{\#\#}$P<0.01 and $^{\#\#\#}$P<0.001 vs. gCTRP3 group. gCTRP3, globular C1q/tumor necrosis factor-related protein 3; ALP, alkaline phosphatase; ARS, Alizarin red staining; RUNX2, Runt-related transcription factor-2; OCN, osteocalcin.

of osteoprotegerin in osteoblasts, reduces the expression of RANKL and indirectly inhibits osteoclast differentiation (51). The results of the present study revealed that AMPK inhibition reduced ALP activity, osteoblast differentiation and mineralized calcium nodules of MC3T3-E1 cells.

SIRT1 is involved in intracellular energy metabolism via the AMPK signaling pathway, and modulates bone metabolism in an AMPK-dependent manner. Wang *et al* (52) revealed that AMPK promotes the osteogenic differentiation of pre-osteoblast MC3T3-E1 cells through the AMPK/GFI1/OPN pathway, and the osteogenic differentiation of AMPKα2-overexpressed cell models has been shown to be markedly increased. Notably, AMPK facilities bone metabolism via activation of SIRT1, which deacetylates and activates the kinase upstream of AMPK, LKB1. In addition, AMPK activation increases the NAD^+/NADH ratio and further activates SIRT1 (53). Notably, it has been reported that cholesterol sulfate inhibits osteoclast differentiation and survival by activating the AMPK/SIRT1

axis (54). El-Haj *et al* (55) revealed that SIRT1 expression levels are markedly reduced in the bone tissue of female patients with osteoporotic fractures. Moreover, treatment with the SIRT1 agonist, SRT3025, significantly reduces the expression levels of osteoblast proteins and maintains the osteogenic differentiation of bone marrow mesenchymal stem cells. The results of the present study indicated that gCTRP3 stimulated the expression of SIRT1, and treatment with the SIRT1 inhibitor, EX527, suppressed ALP activity, osteoblast differentiation and mineralized calcium nodules in MC3T3-E1 cells.

Nrf2 has an important role in regulating bone development and metabolism. During osteoclast formation, inhibition of Nrf2 expression can increase the number of osteoclasts (56). Furthermore, azilsartan ameliorates OVX-induced osteoporosis by activating Nrf2 signaling (46), and anemoside B4 attenuates RANKL-induced osteoclastogenesis by upregulating Nrf2, and dampens OVX-induced bone loss (57). Moreover, Nrf2 overexpression reduces the number of osteoclasts and downregulates RANKL expression (58). In the process of osteogenic differentiation, osteoblasts cannot differentiate in the absence of Nrf2, and osteogenic differentiation is inhibited in the presence of high oxidative stress (59,60). The present study demonstrated that gCTRP3 promoted Nrf2 expression, reduced the number of osteoclasts in OVX-induced mice and promoted the osteogenic differentiation of MC3T3-E1 cells.

In conclusion, gCTRP3 inhibited OVX-induced osteoporosis in mice, and promoted the osteogenic differentiation of MC3T3-E1 cells through increasing ALP activity, osteoblast differentiation and mineralized calcium nodules via activation of the AMPK/SIRT1/Nrf2 signaling pathway. The results of the present study provide a novel theoretical basis for the role of CTRP3 in OVX-induced osteoporosis, and revealed that CTRP3 may exhibit potential as a therapeutic target for the postoperative treatment of OVX-induced osteoporosis.

Acknowledgements

Not applicable.

Funding

This study was supported by the Government Funding for Clinical Medical Excellence of Hebei Province (grant no. ZF2023087). The funders had no role in the study design, data collection and analysis, decision to publish or preparation of the manuscript.

Availability of data and materials

The data generated in the present study may be requested from the corresponding author.

Authors' contributions

XZ and YZha contributed to the conception and design of the study. DZ, JQ, HZ, HQ and FZ contributed to the experiments and generated the figures. XJZ, YZho and YZha analyzed and interpreted data. XZ drafted the manuscript and YZha revised and edited it. All authors read and approved the final version of the manuscript. XZ and YZha confirm the authenticity of all the raw data.

Ethics approval and consent to participate

The present study was approved by the Ethics Committee of The Third Hospital of Hebei Medical University (approval no. Z2023-020-1).

Patient consent for publication

Not applicable.

Competing interests

The authors declare that they have no competing interests.

References

1. Ji MX and Yu Q: Primary osteoporosis in postmenopausal women. Chronic Dis Transl Med 1: 9-13, 2015.
2. Huang YF, Li LJ, Gao SQ, Chu Y, Niu J, Geng FN, Shen YM and Peng LH: Evidence based anti-osteoporosis effects of Periplaneta americana L on osteoblasts, osteoclasts, vascular endothelial cells and bone marrow derived mesenchymal stem cells. BMC Complement Altern Med 17: 413, 2017.
3. Peterson JM, Seldin MM, Wei Z, Aja S and Wong GW: CTRP3 attenuates diet-induced hepatic steatosis by regulating triglyceride metabolism. Am J Physiol Gastrointest Liver Physiol 305: G214-224, 2013.
4. Murayama MA, Kakuta S, Maruhashi T, Shimizu K, Seno A, Kubo S, Sato N, Saijo S, Hattori M and Iwakura Y: CTRP3 plays an important role in the development of collagen-induced arthritis in mice. Biochem Biophys Res Commun 443: 42-48, 2014.
5. Kim MJ, Park EJ, Lee W, Kim JE and Park SY: Regulation of the transcriptional activation of CTRP3 in chondrocytes by c-Jun. Mol Cell Biochem 368: 111-117, 2012.
6. Xu ZH, Zhang X, Xie H, He J, Zhang WC, Jing DF and Luo X: Serum CTRP3 Level is associated with osteoporosis in postmenopausal women. Exp Clin Endocrinol Diabetes 126: 559-563, 2018.
7. Demirtas D, Acıbucu F, Baylan FA, Gulumsek E and Saler T: CTRP3 is significantly decreased in patients with primary hyperparathyroidism and closely related with osteoporosis. Exp Clin Endocrinol Diabetes 128: 152-157, 2020.
8. Youngstrom DW, Zondervan RL, Doucet NR, Acevedo PK, Sexton HE, Gardner EA, Anderson JS, Kushwaha P, Little HC, Rodriguez S, *et al*: CTRP3 regulates endochondral ossification and bone remodeling during fracture healing. J Orthop Res 38: 996-1006, 2020.
9. Kim JY, Min JY, Baek JM, Ahn SJ, Jun HY, Yoon KH, Choi MK, Lee MS and Oh J: CTRP3 acts as a negative regulator of osteoclastogenesis through AMPK-c-Fos-NFATc1 signaling in vitro and RANKL-induced calvarial bone destruction in vivo. Bone 79: 242-251, 2015.
10. Zhou Y, Wang JY, Feng H, Wang C, Li L, Wu D, Lei H, Li H and Wu LL: Overexpression of c1q/tumor necrosis factor-related protein-3 promotes phosphate-induced vascular smooth muscle cell calcification both in vivo and in vitro. Arterioscler Thromb Vasc Biol 34: 1002-1010, 2014.
11. Wang N, Wang L, Yang J, Wang Z and Cheng L: Quercetin promotes osteogenic differentiation and antioxidant responses of mouse bone mesenchymal stem cells through activation of the AMPK/SIRT1 signaling pathway. Phytother Res 35: 2639-2650, 2021.
12. Li Z, Chen C, Zhu X, Li Y, Yu R and Xu W: Glycyrrhizin Suppresses RANKL-Induced Osteoclastogenesis and Oxidative Stress Through Inhibiting NF-κB and MAPK and Activating AMPK/Nrf2. Calcif Tissue Int 103: 324-337, 2018.
13. Yan Z, Cao X, Wang C, Liu S, Li Y, Lu G, Yan W, Guo R, Zhao D, Cao J and Xu Y: C1q/tumor necrosis factor-related protein-3 improves microvascular endothelial function in diabetes through the AMPK/eNOS/NO signaling pathway. Biochem Pharmacol 195: 114745, 2022.

14. Li Y, Wright GL and Peterson JM: C1q/TNF-Related Protein 3 (CTRP3) function and regulation. Compr Physiol 7: 863-878, 2017.
15. Kirketerp-Møller N, Bayarri-Olmos R, Krogfelt KA and Garred P: C1q/TNF-related protein 6 is a pattern recognition molecule that recruits collectin-11 from the complement system to ligands. J Immunol 204: 1598-1606, 2020.
16. Omeka WKM, Liyanage DS, Priyathilaka TT, Kwon H, Lee S and Lee J: Characterization of four C1q/TNF-related proteins (CTRPs) from red-lip mullet (Liza haematocheila) and their transcriptional modulation in response to bacterial and pathogen-associated molecular pattern stimuli. Fish Shellfish Immunol 84: 158-168, 2019.
17. Wu L, Gao L, Zhang D, Yao R, Huang Z, Du B, Wang Z, Xiao L, Li P, Li Y, *et al*: C1QTNF1 attenuates angiotensin II-induced cardiac hypertrophy via activation of the AMPKa pathway. Free Radic Biol Med 121: 215-230, 2018.
18. Mu Y, Yin TL, Yin L, Hu X and Yang J: CTRP3 attenuates high-fat diet-induced male reproductive dysfunction in mice. Clin Sci (Lond) 132: 883-899, 2018.
19. Zhang CL, Feng H, Li L, Wang JY, Wu D, Hao YT, Wang Z, Zhang Y and Wu LL: Globular CTRP3 promotes mitochondrial biogenesis in cardiomyocytes through AMPK/PGC-1α pathway. Biochim Biophys Acta Gen Subj 1861: 3085-3094, 2017.
20. Sudo H, Kodama HA, Amagai Y, Yamamoto S and Kasai S: In vitro differentiation and calcification in a new clonal osteogenic cell line derived from newborn mouse calvaria. J Cell Biol 96: 191-198, 1983.
21. Yang N, Zhang X, Li L, Xu T, Li M, Zhao Q, Yu J, Wang J and Liu Z: Ginsenoside Rc promotes bone formation in ovariectomy-induced osteoporosis in vivo and osteogenic differentiation in vitro. Int J Mol Sci 23: 6187, 2022.
22. Park CH, Lee B, Han M, Rhee WJ, Kwak MS, Yoo TH and Shin JS: Canagliflozin protects against cisplatin-induced acute kidney injury by AMPK-mediated autophagy in renal proximal tubular cells. Cell Death Discov 8: 12, 2022.
23. Qin H, Zhang H, Zhang X, Zhang S, Zhu S and Wang H: Resveratrol protects intestinal epithelial cells against radiation-induced damage by promoting autophagy and inhibiting apoptosis through SIRT1 activation. J Radiat Res 62: 574-581, 2021.
24. Wang Z, Han N, Zhao K, Li Y, Chi Y and Wang B: Protective effects of pyrroloquinoline quinine against oxidative stress-induced cellular senescence and inflammation in human renal tubular epithelial cells via Keap1/Nrf2 signaling pathway. Int Immunopharmacol 72: 445-453, 2019.
25. Livak KJ and Schmittgen TD: Analysis of relative gene expression data using real-time quantitative PCR and the 2(-Delta Delta C(T)) method. Methods 25: 402-408, 2001.
26. Tripathi A, John AA, Kumar D, Kaushal SK, Singh DP, Husain N, Sarkar J and Singh D: MiR-539-3p impairs osteogenesis by suppressing Wnt interaction with LRP-6 co-receptor and subsequent inhibition of Akap-3 signaling pathway. Front Endocrinol (Lausanne) 13: 977347, 2022.
27. Park OJ, Kwon Y, Kim J, Park C, Yun CH and Han SH: Muramyl dipeptide alleviates estrogen deficiency-induced osteoporosis through canonical Wnt signaling. J Pathol 260: 137-147, 2023.
28. Xu H, Xu J, Chen F, Liu T, Li J, Jiang L, Jia Y, Hu C, Gao Z, Gan C, *et al*: Acanthopanax senticosus aqueous extract ameliorates ovariectomy-induced bone loss in middle-aged mice by inhibiting the receptor activator of nuclear factor-κB ligand-induced osteoclastogenesis. Food Funct 11: 9696-9709, 2020.
29. Maeda T, Jikko A, Abe M, Yokohama-Tamaki T, Akiyama H, Furukawa S, Takigawa M and Wakisaka S: Cartducin, a paralog of Acrp30/adiponectin, is induced during chondrogenic differentiation and promotes proliferation of chondrogenic precursors and chondrocytes. J Cell Physiol 206: 537-544, 2006.
30. Yokohama-Tamaki T, Maeda T, Tanaka TS and Shibata S: Functional analysis of CTRP3/cartducin in Meckel's cartilage and developing condylar cartilage in the fetal mouse mandible. J Anat 218: 517-533, 2011.
31. Zhao G, Zhang L, Qian D, Sun Y and Liu W: miR-495-3p inhibits the cell proliferation, invasion and migration of osteosarcoma by targeting C1q/TNF-related protein 3. Onco Targets Ther 12: 6133-6143, 2019.
32. Hou M, Liu J, Liu F, Liu K and Yu B: C1q tumor necrosis factor-related protein-3 protects mesenchymal stem cells against hypoxia- and serum deprivation-induced apoptosis through the phosphoinositide 3-kinase/Akt pathway. Int J Mol Med 33: 97-104, 2014.
33. Vimalraj S: Alkaline phosphatase: Structure, expression and its function in bone mineralization. Gene 754: 144855, 2020.
34. Sharma U, Pal D and Prasad R: Alkaline phosphatase: An overview. Indian J Clin Biochem 29: 269-278, 2014.
35. Komori T: Molecular mechanism of runx2-dependent bone development. Mol Cells 43: 168-175, 2020.
36. Zhang K, Qiu W, Li H, Li J, Wang P, Chen Z, Lin X and Qian A: MACF1 overexpression in BMSCs alleviates senile osteoporosis in mice through TCF4/miR-335-5p signaling pathway. J Orthop Translat 39: 177-190, 2023.
37. Siqueira R, Ferreira JA, Rizzante FAP, Moura GF, Mendonça DBS, de Magalhães D, Cimões R and Mendonça G: Hydrophilic titanium surface modulates early stages of osseointegration in osteoporosis. J Periodontal Res 56: 351-362, 2021.
38. Qin X, Jiang Q, Komori H, Sakane C, Fukuyama R, Matsuo Y, Ito K, Miyazaki T and Komori T: Runt-related transcription factor-2 (Runx2) is required for bone matrix protein gene expression in committed osteoblasts in mice. J Bone Miner Res 36: 2081-2095, 2021.
39. Yu X, Liu S, Dong K and Liu Z: The effects of p38MAPK inhibitor SB203580 on MC3T3-E1 cell proliferation and differetiation under high glucose concentration. J Pract Stomatology 31: 184-187, 2015.
40. Kim SG, Kim JR and Choi HC: Quercetin-Induced AMP-Activated protein kinase activation attenuates vasoconstriction through LKB1-AMPK signaling pathway. J Med Food 21: 146-153, 2018.
41. Su Q, Peng M, Zhang Y, Xu W, Darko KO, Tao T, Huang Y, Tao X and Yang X: Quercetin induces bladder cancer cells apoptosis by activation of AMPK signaling pathway. Am J Cancer Res 6: 498-508, 2016.
42. Kim GT, Lee SH and Kim YM: Quercetin Regulates Sestrin 2-AMPK-mTOR signaling pathway and induces apoptosis via increased intracellular ROS in HCT116 colon cancer cells. J Cancer Prev 18: 264-270, 2013.
43. Wang Y, Viollet B, Terkeltaub R and Liu-Bryan R: AMP-activated protein kinase suppresses urate crystal-induced inflammation and transduces colchicine effects in macrophages. Ann Rheum Dis 75: 286-294, 2016.
44. Li Y, Su J, Sun W, Cai L and Deng Z: AMP-activated protein kinase stimulates osteoblast differentiation and mineralization through autophagy induction. Int J Mol Med 41: 2535-2544, 2018.
45. Huang Y, Yao H, Tjahjono AW, Xiang L, Li K, Tang J and Gao Y: Si-Zhi Wan regulates osteoclast autophagy in osteoporosis through the AMPK signaling pathway to attenuate osteoclastogenesis. J Pharm Pharmacol 76: 236-244, 2024.
46. Cho KM, Kim YS, Lee M, Lee HY and Bae YS: Isovaleric acid ameliorates ovariectomy-induced osteoporosis by inhibiting osteoclast differentiation. J Cell Mol Med 25: 4287-4297, 2021.
47. Dasgupta B and Seibel W: Compound C/Dorsomorphin: Its use and misuse as an AMPK inhibitor. Methods Mol Biol 1732: 195-202, 2018.
48. Langelueddecke C, Jakab M, Ketterl N, Lehner L, Hufnagl C, Schmidt S, Geibel JP, Fuerst J and Ritter M: Effect of the AMP-kinase modulators AICAR, metformin and compound C on insulin secretion of INS-1E rat insulinoma cells under standard cell culture conditions. Cell Physiol Biochem 29: 75-86, 2012.
49. Su CW, Chang YC, Chien MH, Hsieh YH, Chen MK, Lin CW and Yang SF: Loss of TIMP3 by promoter methylation of Sp1 binding site promotes oral cancer metastasis. Cell Death Dis 10: 793, 2019.
50. Kang H, Viollet B and Wu D: Genetic deletion of catalytic subunits of AMP-activated protein kinase increases osteoclasts and reduces bone mass in young adult mice. J Biol Chem 288: 12187-12196, 2013.
51. Mai QG, Zhang ZM, Xu S, Lu M, Zhou RP, Zhao L, Jia CH, Wen ZH, Jin DD and Bai XC: Metformin stimulates osteoprotegerin and reduces RANKL expression in osteoblasts and ovariectomized rats. J Cell Biochem 112: 2902-2909, 2011.
52. Wang YG, Han XG, Yang Y, Qiao H, Dai KR, Fan QM and Tang TT: Functional differences between AMPK α1 and α2 subunits in osteogenesis, osteoblast-associated induction of osteoclastogenesis, and adipogenesis. Sci Rep 6: 32771, 2016.
53. Cetrullo S, D'Adamo S, Tantini B, Borzi RM and Flamigni F: mTOR, AMPK, and Sirt1: Key players in metabolic stress management. Crit Rev Eukaryot Gene Expr 25: 59-75, 2015.
54. Park JH, Lee J, Lee GR, Kwon M, Lee HI, Kim N, Kim HJ, Lee MO and Jeong W: Cholesterol sulfate inhibits osteoclast differentiation and survival by regulating the AMPK-Sirt1-NF-κB pathway. J Cell Physiol 238: 2063-2075, 2023.

55. El-Haj M, Gurt I, Cohen-Kfir E, Dixit V, Artsi H, Kandel L, Yakubovsky O, Safran O and Dresner-Pollak R: Reduced Sirtuin1 expression at the femoral neck in women who sustained an osteoporotic hip fracture. Osteoporos Int 27: 2373-2378, 2016.
56. Han J, Yang K, An J, Jiang N, Fu S and Tang X: The Role of NRF2 in Bone Metabolism-Friend or Foe? Front Endocrinol (Lausanne) 13: 813057, 2022.
57. Cao Z, Niu X, Wang M, Yu S, Wang M, Mu S, Liu C and Wang Y: Anemoside B4 attenuates RANKL-induced osteoclastogenesis by upregulating Nrf2 and dampens ovariectomy-induced bone loss. Biomed Pharmacother 167: 115454, 2023.
58. Kanzaki H, Shinohara F, Kajiya M and Kodama T: The Keap1/Nrf2 protein axis plays a role in osteoclast differentiation by regulating intracellular reactive oxygen species signaling. J Biol Chem 288: 23009-23020, 2013.
59. Sun YX, Li L, Corry KA, Zhang P, Yang Y, Himes E, Mihuti CL, Nelson C, Dai G and Li J: Deletion of Nrf2 reduces skeletal mechanical properties and decreases load-driven bone formation. Bone 74: 1-9, 2015.
60. Pitoniak A and Bohmann D: Mechanisms and functions of Nrf2 signaling in Drosophila. Free Radic Biol Med 88: 302-313, 2015.